



# Prosthetic Visual Acuity with the PRIMA Subretinal Microchip in Patients with Atrophic Age-Related Macular Degeneration at 4 Years Follow-up

Mahiul Muhammed Khan Muqit, MD, FRCOphth,<sup>1,2,\*</sup> Yannick Le Mer, MD,<sup>3,4,\*</sup> Lisa Olmos de Koo, MD,<sup>5</sup> Frank G. Holz, MD,<sup>6</sup> Jose A. Sahel, MD,<sup>3,4,7</sup> Daniel Palanker, PhD<sup>8</sup>

**Objective:** To assess the efficacy and safety of the PRIMA neurostimulation system with a subretinal microchip for improving visual acuity (VA) in patients with geographic atrophy (GA) due to age-related macular degeneration (AMD) at 48-months postimplantation.

**Design:** Feasibility clinical trial of the PRIMA subretinal prosthesis in patients with atrophic AMD, measuring best-corrected ETDRS VA ([Clinicaltrials.gov](https://clinicaltrials.gov/NCT03333954) NCT03333954).

**Subjects:** Five patients with GA, no foveal light perception, and VA of logarithm of the minimum angle of resolution (logMAR) 1.3 to 1.7 (20/400-20/1000) in their worse-seeing “study” eye.

**Methods:** In patients subretinally implanted with a photovoltaic neurostimulation array containing 378 pixels of 100  $\mu\text{m}$  in size, the VA was measured with and without the PRIMA system using ETDRS charts at 1 m. The system’s external components, augmented reality glasses, and pocket computer provide image processing capabilities, including zoom.

**Main Outcome Measures:** Visual acuity using ETDRS charts with and without the system, as well as light sensitivity in the central visual field, measured by Octopus perimetry. Anatomical outcomes demonstrated by fundus photography and OCT up to 48 months postimplantation.

**Results:** All 5 subjects met the primary end point of light perception elicited by the implant in the scotoma area. In 1 patient, the implant was incorrectly inserted into the choroid. One subject died 18 months post-implantation due to study-unrelated reasons. ETDRS VA results for the remaining 3 subjects are reported here. Without zoom, VA closely matched the pixel size of the implant:  $1.17 \pm 0.13$  pixels, corresponding to a mean logMAR of 1.39, or Snellen of 20/500, ranging from 20/438 to 20/565. Using zoom at 48 months, subjects improved their VA by 32 ETDRS letters versus baseline (standard error 5.1) 95% confidence intervals (13.4, 49.9;  $P < 0.0001$ ). Natural peripheral visual function in the treated eye did not decline after surgery or during the 48-month follow-up period ( $P = 0.08$ ).

**Conclusions:** Subretinal implantation of PRIMA in subjects with GA experiencing profound vision loss due to AMD is feasible and well tolerated, with no reduction of natural peripheral vision up to 48 months. Prosthetic central vision provided by photovoltaic neurostimulation enabled patients to reliably recognize letters and sequences of letters, and with zoom, it improved VA of up to 8 ETDRS lines.

**Financial Disclosure(s):** Proprietary or commercial disclosure may be found in the Footnotes and Disclosures at the end of this article. *Ophthalmology Science* 2024;4:100510 © 2024 Published by Elsevier Inc. on behalf of the American Academy of Ophthalmology. This is an open access article under the CC BY-NC-ND license (<http://creativecommons.org/licenses/by-nc-nd/4.0/>).



Supplemental material available at [www.ophtalmologyscience.org](http://www.ophtalmologyscience.org).

Age-related macular degeneration (AMD) is a leading cause of irreversible vision loss associated with increasing age.<sup>1</sup> It was projected to affect 196 million people by 2020.<sup>2</sup> The late and advanced forms of AMD, macular neovascularization (MNV), and geographic atrophy (GA), are associated with severe visual impairment<sup>1–3</sup> and affect 1.49% of the US population aged > 40 years, corresponding to a prevalence rate of approximately 0.94%.<sup>3</sup>

Geographic atrophy, which affects approximately 8 million people worldwide,<sup>4</sup> is associated with a gradual loss of photoreceptors in the macula, encompassing the center, responsible for high-resolution vision. This can severely impair visual functions, such as reading and face recognition. Low-resolution peripheral vision is retained in this condition, necessitating the use of eccentric fixation. Therefore, any treatment strategy to provide functional

central vision should not jeopardize the surrounding healthy retina.

Although photoreceptors are lost within GA, the inner retinal neurons largely survive.<sup>5</sup> PRIMA is a wireless subretinal prosthesis in which photovoltaic pixels directly convert projected light into patterns of electric current<sup>6,7</sup> to reintroduce visual information into the degenerate retina by electrical stimulation of second-order neurons, the bipolar cells.

Preclinical studies in rodents have demonstrated that such stimulation results in a network-mediated retinal response, which preserves many features of normal vision: flicker fusion at high frequencies ( $> 20$  Hz)<sup>6,8</sup> with adaptation to static images,<sup>9</sup> “on” and “off” responses to increments and decrements in light with antagonistic center-surround,<sup>9</sup> and nonlinear summation of the inputs from bipolar cells into ganglion cells’ receptive fields (called subunits),<sup>10</sup> essential for high-spatial resolution.

The first and current version of this implant (PRIMA, Pixium Vision) is 2 mm wide (corresponding to about  $7^\circ$  of the visual angle in a human eye) and  $30\ \mu\text{m}$  thick chip, containing 378 pixels of  $100\ \mu\text{m}$  in width (Fig 1). Images captured by the camera on augmented reality (AR) glasses are processed and projected onto the implant (Fig 2) using near-infrared (880 nm) light to avoid the photophobic and phototoxic effects of bright illumination.<sup>11</sup> Photovoltaic pixels convert this light into electric current flowing through the retina between the active and return electrodes, which stimulates the nearby inner retinal neurons.<sup>7</sup> Their responses then pass through the retinal neural network to ganglion cells, thereby harnessing the residual retinal signal processing.<sup>6,10,12</sup> To avoid irreversible electrochemical reactions at the electrode–electrolyte interface, stimulation is pulsed and charge-balanced.<sup>13</sup> For a steady perception under pulsed illumination, sufficiently high frequencies (30 Hz) are applied to enable flicker fusion.

The electric field is highly localized because of the presence of the active and return electrodes in each pixel<sup>6</sup>: preclinical testing in rodents with  $75\ \mu\text{m}$  and  $55\ \mu\text{m}$  pixels demonstrated grating acuity matching the pixel pitch.<sup>6,14</sup> Perceptual tests of the PRIMA implants with  $100\ \mu\text{m}$  pixels in nonhuman primates demonstrated stimulation thresholds similar to those observed in rodents and responses (saccadic movement) down to a single pixel activation.<sup>15</sup>

To assess prosthetic vision independently of the remaining natural vision in the first phase of the study, opaque (virtual reality) glasses were used. The initial primary efficacy end point was the light perception at the implant location, assessed by an Octopus 900 perimeter (Haag-Streit). The 12-month results, reported in 2020, demonstrated that submacular implantation of the PRIMA array in patients with GA is feasible, with no decrease in eccentric natural acuity, eliciting visual percepts in the former scotoma through neurostimulation by the implant.<sup>16</sup>

In October 2019, the PRIMA glasses were modified from an opaque (virtual reality) to a transparent (AR) design (Fig 2). This enabled patients to use their natural peripheral vision simultaneously with central prosthetic vision.<sup>17</sup> A

secondary end point was added to the study between 18 and 24 months: measurement of visual acuity (VA) using Landolt C optotypes. Visual acuity was measured in the implanted eye with and without-PRIMA-2 glasses, with and without zoom, allowing magnification levels of  $1\times$ ,  $2\times$ ,  $4\times$ , and  $8\times$ . To distinguish prosthetic vision from the residual natural one, contrast in prosthetic vision was inverted so that subjects typically perceive white letters on a black background. In 2022, we reported the 24-month follow-up results, demonstrating implant stability and Landolt C acuity without zoom closely matching the  $100\ \mu\text{m}$  pixel size:  $1.17 \pm 0.13$  pixels, corresponding to the average of logarithm of the minimum angle of resolution (logMAR) 1.39, or 20/500 on a Snellen scale, ranging from 20/438 to 20/565.<sup>17</sup> We also reported that thickness of the retinal layers remained stable during the 36-months follow-up, with no adverse structural abnormality across the implant.<sup>18</sup>

In 2022, an ETDRS test of VA was added to the protocol as a secondary end point. Here, we report the safety profile and prosthetic vision achieved under these settings at the 4-year follow-up with the PRIMA subretinal microchip and system’s zoom function.

## Methods

### Patients

This feasibility study of the PRIMA implant (NCT03333954) aimed to test safety and functionality in 5 patients with atrophic AMD. The study adhered to the Declaration of Helsinki and received ethical approval from the Comité de Protection des Personnes Ile de France II and the Agence Nationale de Sécurité du Médicament et des Produits de Santé. Study participants were aged  $> 60$  years and had advanced dry AMD with an atrophic zone of at least 3 optic disc diameters and best-corrected VA of  $\leq 20/400$  in the worse-seeing study eye; no foveal light perception (absolute scotoma) but visual perception in the periphery, with preferred retinal locus determined by microperimetry; absence of photoreceptors and presence of the inner retina in the atrophic area, as confirmed by OCT; absence of MNV verified by retinal angiography. All other ocular and general pathologies that could contribute to low VA were excluded. Patients provided written informed consent to participate in the study. Visual acuity in the nonimplanted fellow eye was measured throughout the study as a control. Surgical procedures were performed in the Fondation Ophtalmologique A. de Rothschild (Paris, France), with the first subject implanted in December 2017 and the fifth in June 2018.<sup>18</sup> The patients’ rehabilitation and visual function assessment was carried out at the clinical Investigation Center of the Quinze-Vingts National Eye Hospital (Paris, France).

### PRIMA Implantation

In a preplanning phase of the implantation, the surgeon (Y.L.M.) examined the fundus images and OCT scans. PRIMA implantation site was determined based on the preferred retinal locus position and atrophy size. The implantation surgery was performed under local anesthesia in 1 case, and under general anesthesia in 4 patients. Complete 23-gauge trans pars plana vitrectomy was performed with peripheral vitreous base shaving. A posterior vitreous detachment was confirmed using intravitreal triamcinolone (Kenalog-40, Bristol Myers Squibb). A 27-gauge chandelier and 23-gauge Alcon light pipe were used for intraocular illumination.

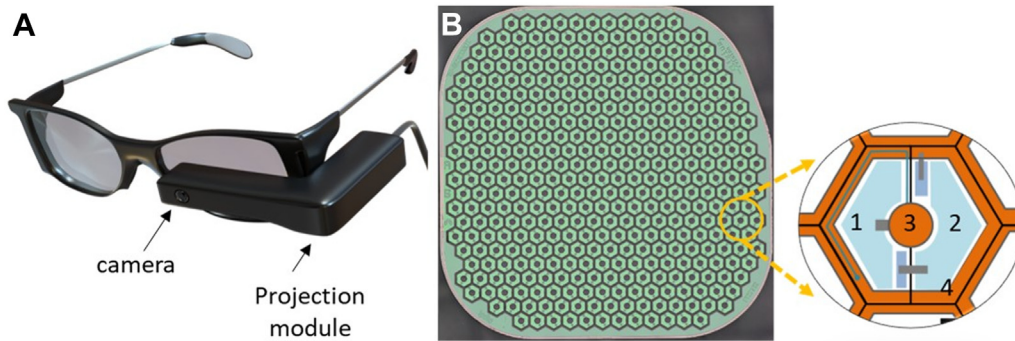


**Figure 1.** PRIMA subretinal microchip neurostimulation system. **A**, Transparent augmented reality glasses PRIMA-2; **B**, Implant of  $2 \times 2$  mm in width and  $30 \mu\text{m}$  in thickness, composed of  $100 \mu\text{m}$  wide hexagonal pixels, which include 2 photodiodes (#1, 2) connected between the central active electrode (#3) and a circumferential return electrode (#4).

The retina was detached between the macula and the planned position of the retinotomy by injecting a balanced salt solution with controlled visco fluid injection to form a bleb using a 41-gauge straight needle, at a maximal pressure of 12 pounds per square inch. The location of the sclerotomy was chosen to obtain a straight alignment between the sclerotomy, retinotomy, and the fovea. The detached retina was marked with diathermy. Retinotomy of 2.4 mm in size was created in the temporal area, about 1 mm outside the atrophic retina, using 23-gauge vertical scissors, and then incised on a length of 3 mm at 4 to 5 mm distance from the fovea. Retinotomy location was selected based on preoperative fundus image and microperimetry to reduce the risk of jeopardizing the useful residual vision, including the preferred retinal locus. In 1 case, a localized endodiathermy was needed to stop a retinal vessel bleeding.

A subretinal spatula was used to detach the macula, with care taken to avoid button-holing any thinned areas of the macula and avoid the formation of a full-thickness macular hole. During surgery, the PRIMA implant was delivered through the retinotomy and into the subretinal space at the macula using silicone-tipped forceps. A bubble of perfluorocarbon liquid was injected over the macula to flatten the fluid bleb and stabilize the implant at the submacular docking site during the forceps removal and to close

the retinotomy. The chip was then shifted to its final location near the fovea by careful transretinal manipulation using the blunt side of the subretinal pick to push the edge of the chip slowly under the attached retina. When the chip location was considered to be optimal, intraoperative OCT was used to confirm the correct placement and the contact of the macular retina with the anterior surface of the chip. After moving the implant at this location, perfluorocarbon liquid was fully exchanged with air. The absence of subretinal fluid was confirmed using intraoperative OCT in all cases. An indented peripheral retina examination was performed to check for retinal breaks, and any residual perfluorocarbon liquid was removed with a soft tip cannula. A final tamponade with silicone oil (3 cases), 1 case hexafluoroethane ( $\text{C}_2\text{F}_6$ ), and 1 case with sulfur hexafluoride ( $\text{SF}_6$ ) was achieved. All subjects were instructed to posture face-down after surgery to stabilize the retina for 24 hours. Postoperatively, silicone oil removal was carried out 4 weeks after the first operation using the 25G pars plana vitrectomy technique in 2 subjects.

### Assessment of Natural VA

The best-corrected natural VA of each patient was measured without the PRIMA glasses to assess any potential VA changes

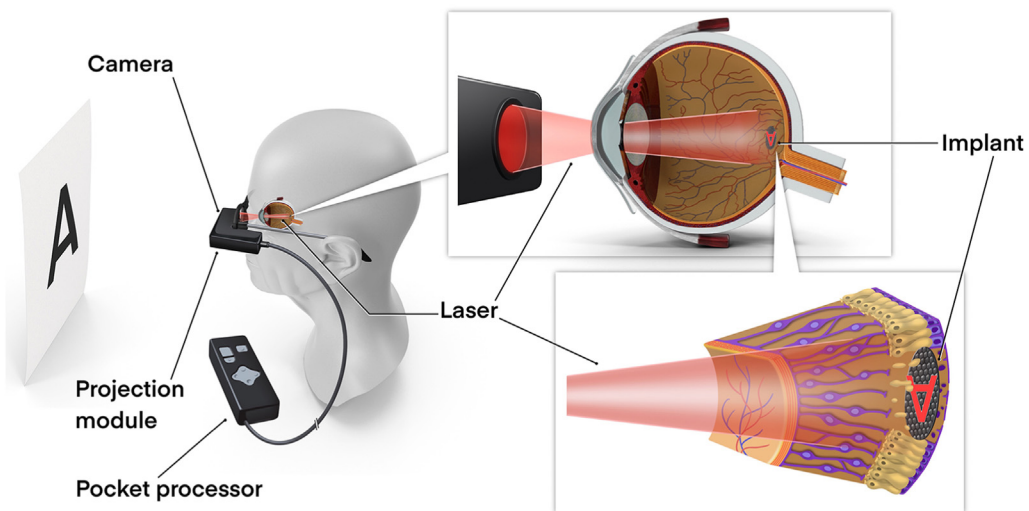


**Figure 2.** Simplified diagram of the PRIMA-2 system. Implant in the subretinal space in 1 eye, camera, and projection module mounted on a pair of glasses, and pocket image processor.



after implantation and over time. ETDRS letter charts were used at 4 m; if the patient could not correctly identify at least 20 letters at 4 m, the test continued at 1 m. The smallest font size for which the patient could read at least 4 letters in 1 line was recorded.

### Assessment of Prosthetic Vision

A camera on the PRIMA-2 AR glasses captured a visual field of  $50^\circ \times 40^\circ$ , with a central third of the image being projected onto the retina to match the display's  $17^\circ$  field of view without zoom. The projected images covered a field of 5.1 mm ( $17^\circ$ ) on the retina, with a resolution of 10.5  $\mu\text{m}$ . Maximum peak retinal irradiance was 3.5  $\text{Mw}/\text{mm}^2$ , with a maximum pulse duration of 10 ms and frame rate of 30 Hz, well within the thermal safety limits for chronic use of near-infrared light.<sup>19</sup> Computer-generated images could also be projected on the ocular display directly, without the use of the camera. The angular magnification of the system without zoom was 1:1. In the measurements of letter recognition, patients were also allowed to use the electronic zoom at their preferred level of magnification ( $1\times$ ,  $2\times$ ,  $3\times$ , or  $8\times$ ), and this setting was recorded.

Visual acuity measurements were performed up to 3 times on different days near the 48-month follow-up, and results are reported as the median of these 3 measurements. The subject was asked to read as many letters as possible from top to bottom on the ETDRS chart placed at 1 meter. The baseline VA test without-PRIMA glasses was also performed at 1 meter but only once because at the time it was not defined as an efficacy end point.

### Assessment of Safety

Investigators reported all the adverse events. These were categorized as serious or nonserious, and whether they were related to the procedure or a device. During follow-up, investigator assessments were reviewed by a clinical events committee.

### Data Synthesis and Analysis

To estimate the mean VA within the study settings, a mixed regression model with random effect for subjects was used.<sup>20</sup> This corresponds to the regression model with logMAR and ETDRS VA as output variables for natural and prosthetic vision, respectively, study setting as input variable, and random effects for subjects. The estimates are reported as standard error (SE) for the mean, 95% confidence intervals (CIs) for the mean, and SE for the mean difference and 95% CI for the mean difference. The estimated means were then compared between study settings using the post hoc Tukey method. The adjusted  $P$  value of  $< 0.05$  was considered statistically significant. The analysis was performed using R version 4.1.2.<sup>21</sup>

To test changes within the study and nonstudy eyes, as well as to compare the possible differences between them, a mixed regression model was developed with VA as output variable; time, eye status (study eye and nonstudy eye), and interaction of time with eye status as input variables; and, finally, with subject as a random effect.

## Results

The first patient was enrolled at the Rothschild Foundation and Quinze-Vingts National Eye Hospital in November 2017 and the last in May 2018. Details of the PRIMA implantation surgery have been published earlier.<sup>11,16,18</sup> Analysis of VA at 4 years was possible for 3 of the 5 patients. All the implants remained stable and functional in the subretinal space (Fig 3). Two patients were

excluded (Fig 4): 1 died from cancer, unrelated to the study, with no data available after the 12-month visit, and the other received an intrachoroidal implantation in error. A summary of demographic data is shown in Table 1, and baseline data were published earlier.<sup>16</sup>

### Natural Vision

During the 48-month follow-up, all subjects experienced a slight reduction of VA in the nonstudy eye, albeit not significant. For all 5 patients, the mean baseline VA in the nonstudy eyes was a logMAR of 0.78 (SE, 0.13; 95% CI, 0.41–1.15) or 20/120, and, in the study eyes, it was a logMAR of 1.48 (SE, 0.13; 95% CI, 1.11–1.85) or 20/600 ( $P < 0.001$ ). At the 48-month visit, in the nonstudy eyes, the estimated mean VA was a logMAR of 1.03 (SE, 0.14; 95% CI, 0.63–1.42) or 20/215; in the study eyes, the mean VA was logMAR 1.33 (SE, 0.14; 95% CI, 0.93–1.72) or 20/430 ( $P = 0.058$ ). Residual natural VA in the treated eye of any patient did not decrease during the 48-month follow-up period. It even exhibited a temporary improvement, albeit not significant:  $P = 0.8$  (Fig 5). By 48 months, the mean VA in the study eyes improved by 0.1 logMAR mainly because of 1 subject who improved by up to a logMAR of 0.4, whereas in other subjects it improved by no more than a logMAR of 0.1.

### Prosthetic Vision

The PRIMA system inverted the contrast of the ETDRS chart so that black letters on a whiteboard are projected as bright stimulation patterns on a black background. As shown in Figure 6, VA improved in all 3 subjects compared with the baseline, and their prosthetic vision (with the PRIMA glasses) was better than their natural vision (without-PRIMA glasses). The means for each setting are as follows: baseline, 11.7 ETDRS letters (SE, 4.8; 95% CI, 0–32.1) or 20/584; without-PRIMA glasses at 48 months, 18.2 ETDRS letters (SE, 4.8; 95% CI, 0–38.6) or 20/433; and with-PRIMA glasses (prosthetic vision with preferred magnification) at 48 months, 43.3 ETDRS letters (SE, 4.8; 95% CI, 22.9–63.8) or 20/136.

The differences between the settings were as follows: natural vision at 48 months (without-PRIMA glasses) compared with the baseline, +6.5 ETDRS letters (SE 5.1; 95% CI, –11.7 to 24.7;  $P = 0.480$ ); prosthetic vision (with-PRIMA glasses) compared with the baseline, +31.7 ETDRS letters (SE, 5.1; 95% CI, 13.4–49.9;  $P = 0.008$ ); and prosthetic vision compared with natural vision at 48 months (with-PRIMA versus without-PRIMA glasses), +25.2 ETDRS letters (SE, 5.1; 95% CI, 6.9–43.4;  $P = 0.017$ ). Both differences, between prosthetic vision and baseline, as well as between prosthetic vision and natural vision at 48 months, are significant. The magnification/zoom range for each participant was as follows: patient 1 ( $1-8\times$ ); patient 2 ( $1-8\times$ ); and patient 3 ( $1-4\times$ ) magnification.

In addition to objective VA measurements, subjects were observed during training sessions. Given their ability to recognize letters, they were able to read sequences of letters and words. This was also observed during exercises, such as reading product names on food packages, panels, and signs

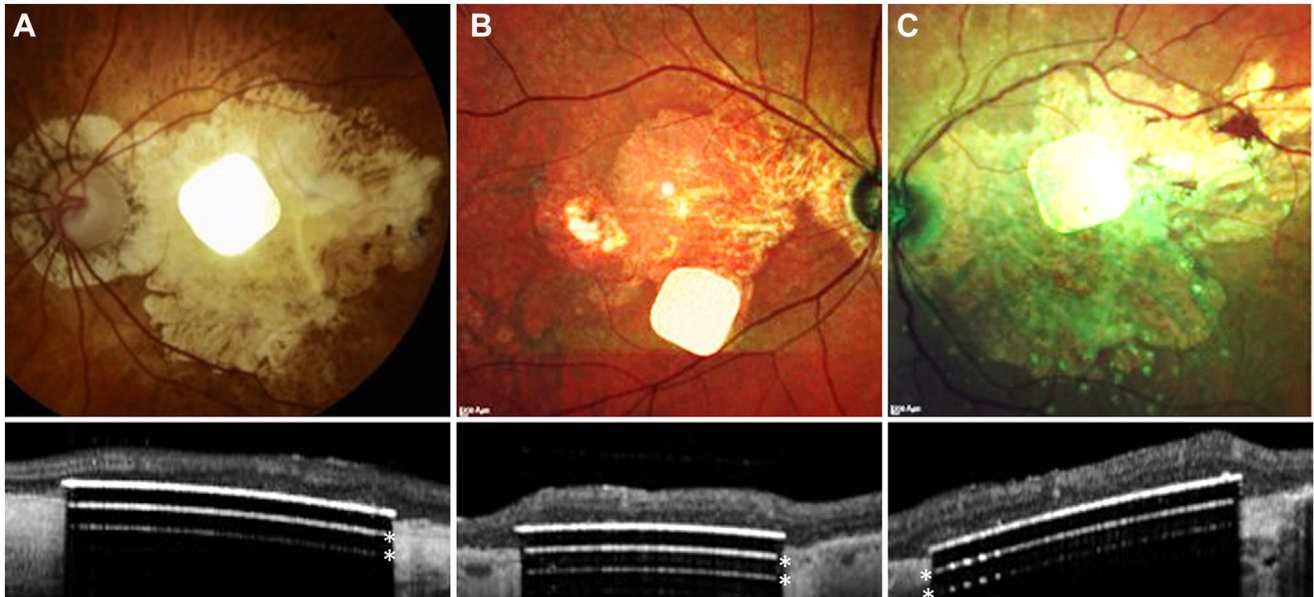


**Figure 3.** Fundus photographs and OCT of the subretinal implants at 48 months in 3 patients (A, B, and C). Two white lines below the implant surface (\*) are the OCT artifacts because of strong light reflection from the implant surface.

outdoors and indoors or a train timetable (Video S1, available at [www.ophtalmologyscience.org](http://www.ophtalmologyscience.org)).

### Safety

In total, 4 study-related serious adverse events were reported in the follow-up of all 5 patients, but none was related to the device (Table 2). Per the investigator assessment, 1 event was definitely procedure-related, 2 were probably

procedure-related, and 1 was possibly procedure-related, as described below. The subject's death because of cancer was neither procedure nor device-related.

The MNV event, which was deemed to be procedure-related, was observed in an area where Bruch's membrane got damaged during implantation surgery under local anesthesia. An unexpected head movement of the subject at the time of retinal implant delivery under the macula led to damage of the Bruch membrane and choroidal hemorrhage.

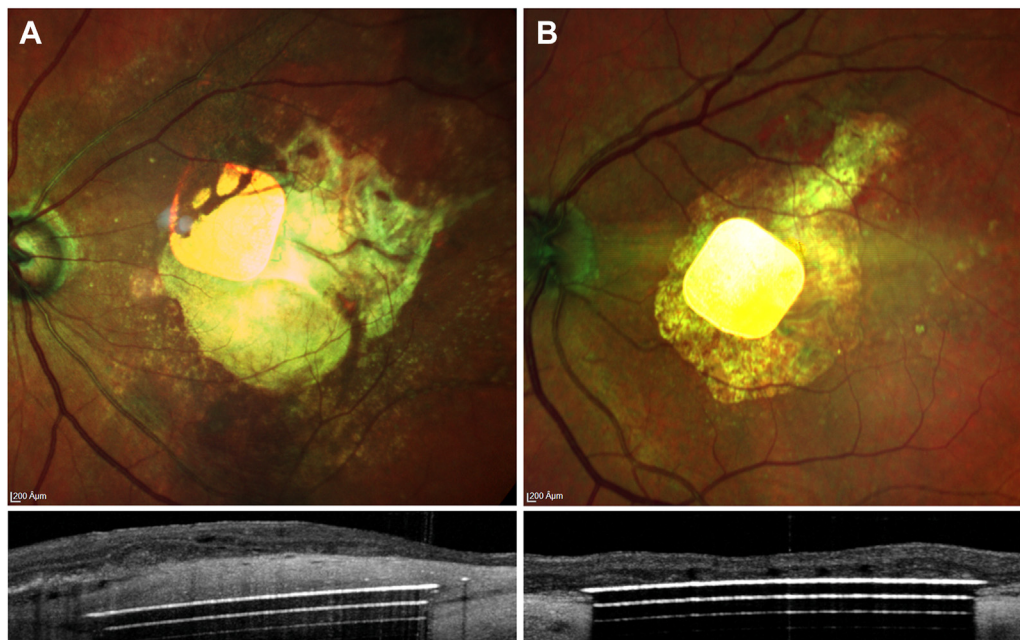


**Figure 4.** Fundus photographs and OCT of the excluded patients at 48 months. A, Implant in the unintended location (inside choroid). B, Implant at 12 months in a deceased patient.

Table 1. Patients Demographics

Age, mean (range), yrs	74.8 (66–83)
Eye implanted	Right eye (1/5) Left eye (4/5)
Gender	Male (2/5) Female (3/5)
Lens at baseline	Pseudophakia (4/5) Phakic (1/5)
Duration of AMD, mean, yrs	7.25

AMD = age-related macular degeneration.

After resorption of blood, fibrotic tissue was observed around the implant which, on OCT, seemed to be located under the pigment epithelium. This patient had visual perception of stimulation but no spatial resolution using the implant, and hence this patient was excluded from the acuity measurements (Fig 4A). Thirty-one months after implantation, an asymptomatic MNV was discovered in the same eye of this subject, within an area that was not touched during surgery. Therefore, it was judged as unlikely to be procedure- or device-related. The MNV was treated with a course of intravitreal ranibizumab injections and resolved after a year without sequelae. At 42 months postimplantation, the same subject developed a second MNV in a different area of the posterior pole near the retinotomy site. This second MNV event was deemed as procedure related.

At 12-months postoperatively, a retinal detachment developed in the control eye of another patient. This was successfully treated with vitrectomy and gas injection, and the retina was reattached. This subject was also known to have underlying glaucoma at baseline and developed uncontrolled ocular hypertension in the implanted eye 2 years

postoperatively, which was unresponsive to medical treatment. The patient underwent a successful trabeculectomy achieving eye pressure control, and treatment remains ongoing. Because vitrectomy risks exacerbation of the pre-existing glaucoma, this adverse event was deemed procedure-related, although the patient already had glaucoma.

All the study-related nonserious adverse events are listed in Table 3. Microcysts were observed in 3 subjects, which resolved without sequelae. The microcysts did not create any symptoms and seemed not to affect the perception of the stimulation by the implant. Two patients developed significant ocular hypertension that required medical treatment.

Implant stability in the subretinal space has been previously reported.<sup>18</sup> The authors have also published data that showed that, in the 3 patients reported in this study, PRIMA implants did not cause any obvious structural changes in the vicinity of the device nor in the outer retinal layers over a 3-year period.<sup>18</sup>

## Discussion

Up to 4 years after implantation, the subretinal microchip activated by PRIMA-2 glasses enabled 3 subjects to read at least 4 additional lines on the vision chart compared with their natural vision. There were some adverse events (serious or not), which were managed efficiently. This did not bring into question the safety and biocompatibility of the device or the patients' ability to tolerate the PRIMA implant.

A key feature of the PRIMA neurostimulation system with a subretinal microchip is the ability of implanted subjects to consistently recognize letters and follow a sequence

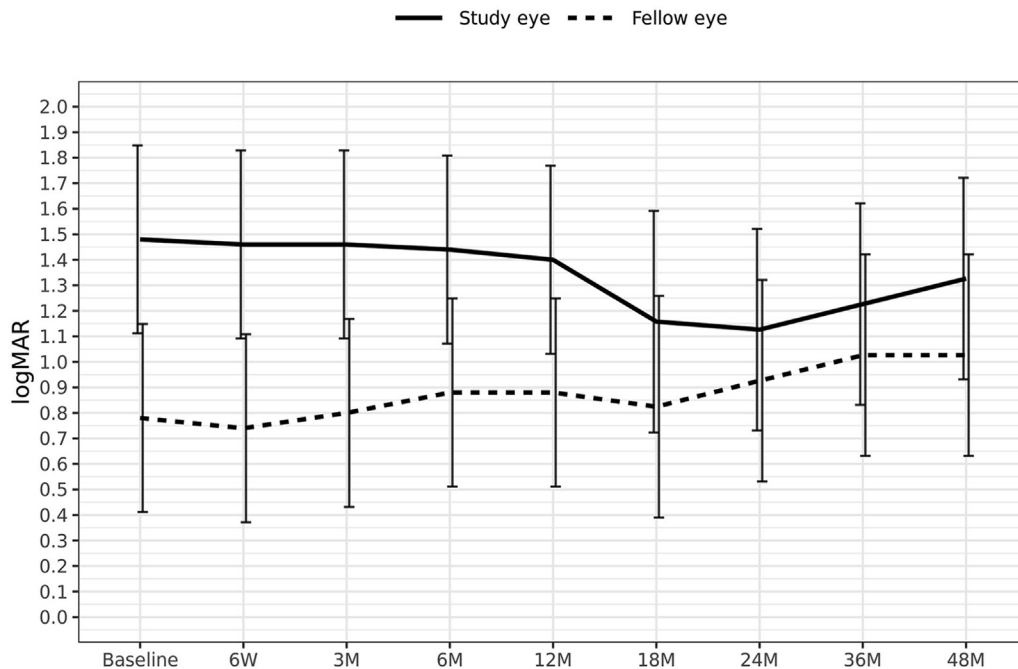


Figure 5. Mean natural visual acuity over time for all patients. Error bars represent confidence intervals. logMAR = logarithm of the minimum angle of resolution.



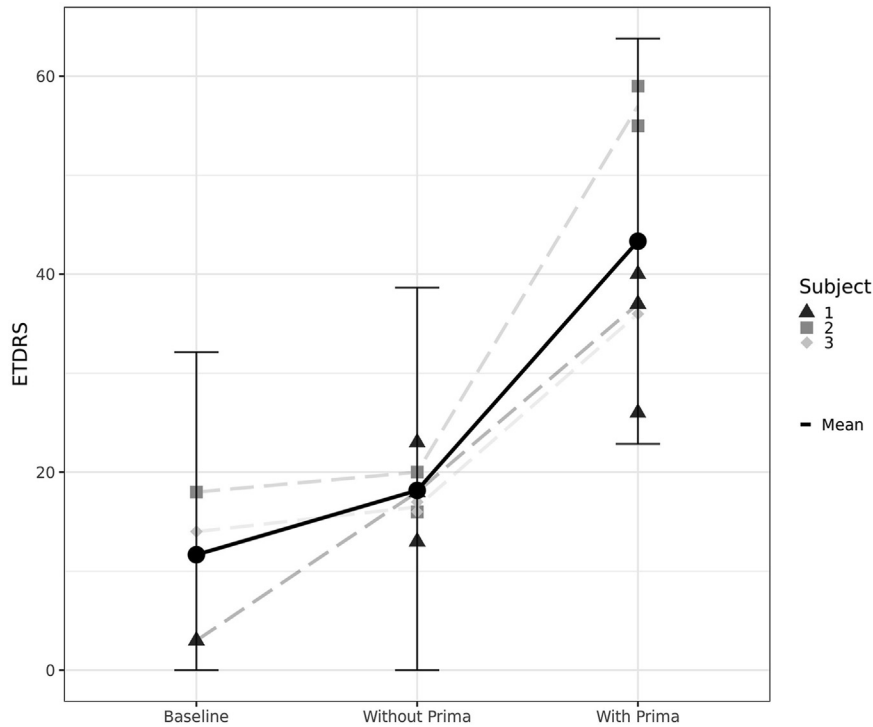


Figure 6. Median best-corrected prosthetic visual acuity with the ETDRS chart at 1 meter distance.

of letters. In this study, all subjects read more letters with PRIMA-2 glasses than without. The difference between prosthetic vision with zoom versus baseline was 32 letters (range of 22 letters to 39 letters). At the 4-year time point, the mean gain was 25 letters, which corresponds to logMAR 0.5 (5 lines). Even without zoom, the PRIMA system compares favorably with the previous epiretinal and sub-retinal prosthetics.<sup>22–26</sup> With zoom, it demonstrated much higher letter acuity, albeit on account of the correspondingly reduced visual field. Such visual gains are clinically meaningful for patients with foveal GA secondary to AMD.

The function of zoom for advanced AMD patients is offered by 2 other technologies: the implanted telescope, such as IMT (VisionCare Ophthalmic Technologies),<sup>27</sup> and Virtual Reality glasses, such as eSight (eSight Eyewear).<sup>28</sup> These 2 devices utilize the preferred retinal locus and peripheral retina and therefore preclude normal use of peripheral vision. To date, neither of these 2 approaches has gained much popularity. PRIMA, on the other hand, enables normal use of residual peripheral vision, while providing central prosthetic vision with optional zoom.

One of the major visual disabilities for patients with advanced AMD and, in particular, with GA is the gradual decline and then a permanent loss of reading ability within the central field.<sup>29–31</sup> Unlike the current pharmacologic treatments for GA, which aim to slow down the growth of atrophic lesions without any functional improvement in VA,<sup>32</sup> our results demonstrate restoration of central vision in the former scotoma.

According to the literature, the expected vision loss due to the progression of GA is up to a logMAR of 1.5 in 5 years.<sup>33,34</sup> Surprisingly, not only the natural VA in the implanted eye did not decrease, but also it temporarily improved in all 3 subjects. The reason for this is unknown. It could be due to a neurotrophic benefit of the subretinal surgery or of the electrical stimulation,<sup>35</sup> or it could be a result of the vision rehabilitation training, which may enhance the gaze control and thus improve the eccentric fixation. However, over time this effect seems to be compromised by the natural degradation of patients' vision.

The vast majority of the device- and procedure-related nonserious adverse events occurred within the first 6 months postimplantation, and none of these events led to

Table 2. Procedure-Related Serious Adverse Events in All 5 Patients

Adverse Event Term	Patients (n)	Device-Related (Definite, Probable, Possible, Not Related)	Procedure-Related (Definite, Probable, Possible, Not Related)	Timing of Onset from Implantation Operation (Mos)
Ocular hypertension	2	Not related	Possible	25
Macular neovascularization	1	Not related	Definite	0 (1 day)
Retinal detachment	1	Not related	Probable	43
			Probable	13

Table 3. Study-Related Nonserious Adverse Events and the Number of Affected Patients

Adverse Event Name	Patients (n)	Device-Related (Definite, Probable, Possible, Not Related, Unlikely)	Procedure-Related (Definite, Probable, Possible, Not Related, Unlikely)	Timing of Onset from Implantation Operation (Mos)
Macular microcyst	3	Unlikely Possible Possible	Possible Possible Possible	12 9.2 2
Ocular hypertension	2	Not related Not related	Probable Probable	0.6 (2.5 wks) 0.7 (3 wks)
Submacular perfluorocarbon liquid bubble	1	Not related	Definite	0
Choroidal hemorrhage	1	Not related	Definite	0
Localized subretinal bleeding	1	Not related	Definite	0
Corneal epithelial defect	1	Not related	Probable	0 (1 day)
Retained silicone oil droplet	1	Not related	Definite	1.2
Punctuate keratitis	1	Not related	Possible	1.6
Headache	1	Not related	Possible	1.7
Myodesopsia	1	Not related	Possible	1.8
Ocular discomfort	1	Not related	Definite	1.4
Peripheral retinal tear	1	Not related	Definite	0
Choroidal detachment in periphery	1	Not related	Definite	0
Vitreous hemorrhage	1	Not related	Probable	0.7 (3 wks)
Subretinal chip displacement	1	Not related	Definite	1
Choroidal neovascularization	1	Unlikely	Unlikely	31

any long-term safety issues. None of the nonserious adverse events, either device- or procedure-related or not, reasonably bring into question the overall safety of the system. These include the microcysts discovered in 3 subjects (2 occurred 9 months postimplantation) and the asymptomatic choroidal neovascular membrane in 1 subject (which occurred 31 months after implantation). Given the small cohort size in this first-in-human study, we can only speculate on the pathophysiology of the microcysts. The most probable explanation would be a mild hyperpermeability inflammatory response after surgery/surgical trauma, which seems to be temporary and nonsignificant. A further hypothesis for the later onset would be one of a microstructural mechanical change in the internal limiting membrane over the zone of the implant, and this may lead to nonexudative microcystic cavitation changes that manifest as microcysts.

There are a number of limitations that we acknowledge for this first-in-human study. The sample size is small, and this reflects a first-in-human study of this kind. The 4-year duration of the follow-up of these patients has been adequate to fully assess the long-term biocompatibility and safety. Zoom function reduces the visual field and hence requires more eye and head scanning. However, patients underwent expert rehabilitation training throughout the trial and became habituated to changes in the visual field with different zoom levels. Regarding visual outcomes with the zoom function, we acknowledge that the baseline VA was not tested with a magnification device. A proper comparison of prosthetic vision to natural vision with optical magnifiers is not trivial because

the latter would affect both central and peripheral vision, whereas prosthetic vision is affected only over the chip inside the scotoma. Although patients could use  $\times 8$  magnification, higher magnifications are unlikely to be convenient, and some patients preferred operating at lower zoom levels.

In summary, the subretinal photovoltaic array provided form vision with letter acuity closely matching the 100  $\mu\text{m}$  pixel size in patients with GA, with no decline in eccentric natural acuity over a 4-year period. The transparent (AR) glasses allow simultaneous use of the prosthetic central and natural peripheral vision. Using electronic zoom, patients demonstrated clinically meaningful and statistically significant improvements in vision. These results were accompanied by an acceptable safety profile. Reduced pixel size in future implants<sup>36,37</sup> may further improve the prosthetic VA to much higher levels.

## Acknowledgments

The authors would like to thank the patients who participated in the study and the Pixium Vision team who designed, fabricated, and tested the PRIMA implant and external components of the neurostimulation system. The authors are also grateful to the scientific and medical advisory board of Pixium Vision for their guidance on the clinical trial design. The authors would also like to acknowledge the scientific, R&D, medical, and clinical research staff who continue the patients' care, rehabilitation, and evaluation. Finally, the authors acknowledge the support within the clinical event committee from Professor Andrea Cusumano and Professor Jan van Meurs.

## Footnotes and Disclosures

Originally received: November 13, 2023.  
Final revision: January 30, 2024.

Accepted: March 4, 2024.

Available online: March 7, 2024. Manuscript no. XOPS-D-23-00282R1.



<sup>1</sup> Vitreoretinal Service, Moorfields Eye Hospital, London, United Kingdom.

<sup>2</sup> Institute of Ophthalmology, University College London, United Kingdom.

<sup>3</sup> Department of Ophthalmology, Fondation Ophtalmologique A. de Rothschild, Paris, France.

<sup>4</sup> Clinical Investigation Center, Quinze-Vingts National Eye Hospital, Paris, France.

<sup>5</sup> Department of Ophthalmology, University of Washington, Seattle, Washington.

<sup>6</sup> Department of Ophthalmology, University of Bonn, Germany.

<sup>7</sup> Department of Ophthalmology, University of Pittsburgh School of Medicine, Pittsburgh, Pennsylvania.

<sup>8</sup> Department of Ophthalmology, Stanford University, Stanford, California.

\*M.M.K.M. and Y.L.M. contributed equally to this work.

Presented the preliminary results of this study were presented at the American Society of Retina Specialists Annual Meeting, July 28, 2023, Seattle, Washington, and the Eye and the Chip conference, October 8, 2023, Detroit, Michigan.

Disclosure(s):

All authors have completed and submitted the ICMJE disclosures form.

The author(s) have made the following disclosure(s):

M.M.K.M.: Consultant – Pixium Vision.

Y.L.M.: Consultant – Pixium Vision.

L.O.D.K.: Consultant – Pixium, Alcon.

F.G.H.: Grants or contracts – Pixium Vision; Consultant – Pixium Vision.

J.A.S.: Support – MTEC W81XWH-22-9-0011, Institut Hospitalo-Universitaire FOReSIGHT (ANR-18-IAHU-0001), NIH National Institutes of Health CORE Grant (P30 EY08098), RPB Research to Prevent Blindness, Unrestricted Grant; Grants or contracts to the institution – European Research Council (ERC) Synergy Helmholtz Grant (#610110), LIGHT4DEAF (ANR-15-RHUS-000), NIH RO1 EY033049; Royalties or licenses – Patents on allotropic expression relevant to gene therapy of Leber hereditary Optic neuropathy, Collected by INSERM from GenSight; Consultant – Avista RX, Tenpoint; Patents planned, issued or pending – Portfolio On Rod-Derived-Cone Viability Factor (Managed By Inserm, Licenced To Sparing Vision), Optogenetic Therapy (Managed By Inserm, Licenced To GenSight); Participation on a Data Safety Monitoring Board or Advisory Board – Unpaid; Leadership or fiduciary role in other board, society, committee or advocacy group, paid or unpaid – Unpaid Censor on the Board Of GenSight, Sparing Vision, Censor on the Board of Avista,

Chair Advisory Board of Sparing Vision, Tenpoint, Institute of Ophthalmology, Basel, President Of Foindation Voir Et Entendre; Director, Board Of Trustees, Rd Fund (Foundation Fighting Blindness), Gilbert Foundation; Stock or stock options – Pixium Vision, GenSight Biologics, Sparing Vision, Prophesee, Chronolife, Tilak Healthcare, VegaVect Inc., Avista, Tenpoint, SharpEye.

D.P.: Royalties or licenses – Pixium Vision (Patent licensing fees to Stanford University); Consulting fees – Pixium Vision.

Supported by Pixium Vision, and in part by the Sight Again project under the Structural R&D Projects for Competitiveness (PSPC) and Investment for the Future (PIA) funding, managed by Bpifrance. D.P. was funded in part by the National Institutes of Health (grant R01-EY027786). The Biomedical Research Centre at Moorfields Eye Hospital, supported in part by the National Institute for Health and Care Research, UK, is also acknowledged. The Clinical Investigation Center at the Quinze-Vingts National Hospital is supported in part by the Inserm-DHOS, France.

HUMAN SUBJECTS: Human subjects were included in this study. The study adhered to the Declaration of Helsinki and received ethical approval from the Comité de Protection des Personnes Ile de France II and the Agence Nationale de Sécurité du Médicament et des Produits de Santé. Patients provided written informed consent to participate in the study.

No animal subjects were used in this study.

Author Contributions:

Conception and design: Muqit, Le Mer, de Koo, Holz, Sahel, Palanker

Data collection: Muqit, Le Mer, de Koo, Holz, Sahel, Palanker

Analysis and interpretation: Muqit, Le Mer, de Koo, Holz, Sahel, Palanker

Obtained funding: N/A

Overall responsibility: Muqit, Le Mer, de Koo, Holz, Sahel, Palanker

Abbreviations and Acronyms:

**AMD** = age-related macular degeneration; **AR** = augmented reality; **CI** = confidence interval; **GA** = geographic atrophy; **logMAR** = logarithm of the minimum angle of resolution; **MNV** = macular neovascularization; **SE** = standard error; **VA** = visual acuity.

Keywords:

Age-related macular degeneration, Geographic atrophy, Neurostimulation, Retinal prosthesis, Subretinal microchip.

Correspondence:

Mahil Muhammed Khan Muqit, MD, FRCOphth, City Road, London, EC1V2PD, United Kingdom. E-mail: [mahi.muqit1@nhs.net](mailto:mahi.muqit1@nhs.net).

## References

- Klein R, Klein BE, Jensen SC, Meuer SM. The five-year incidence and progression of age-related maculopathy: the Beaver Dam Eye Study. *Ophthalmology*. 1997;104:7–21. [https://doi.org/10.1016/s0161-6420\(97\)30368-6](https://doi.org/10.1016/s0161-6420(97)30368-6).
- Wong WL, Su X, Li X, et al. Global prevalence of age-related macular degeneration and disease burden projection for 2020 and 2040: a systematic review and meta-analysis. *Lancet Glob Health*. 2014;2:e106–e116. [https://doi.org/10.1016/S2214-109X\(13\)70145-1](https://doi.org/10.1016/S2214-109X(13)70145-1).
- Rein DB, Wittenborn JS, Burke-Conte Z, et al. Prevalence of Age-related macular degeneration in the US in 2019. *JAMA Ophthalmol*. 2022;140:1202–1208. <https://doi.org/10.1001/jamaophthalmol.2022.4401>.
- Rudnicka AR, Jarrar Z, Wormald R, et al. Age and gender variations in age-related macular degeneration prevalence in populations of European ancestry: a meta-analysis. *Ophthalmology*. 2012;119:571–580. <https://doi.org/10.1016/j.ophtha.2011.09.027>.
- Kim SY, Sadda S, Pearlman J, et al. Morphometric analysis of the macula in eyes with disciform age-related macular degeneration. *Retina*. 2002;22:471–477. <https://doi.org/10.1097/00006982-200208000-00012>.
- Lorach H, Goetz G, Smith R, et al. Photovoltaic restoration of sight with high visual acuity. *Nat Med*. 2015;21:476–482. <https://doi.org/10.1038/nm.3851>.
- Mathieson K, Loudin J, Goetz G, et al. Photovoltaic retinal prosthesis with high pixel density. *Nat Photonics*. 2012;6:391–397. <https://doi.org/10.1038/nphoton.2012.104>.
- Lorach H, Goetz G, Mandel Y, et al. Performance of photovoltaic arrays in-vivo and characteristics of prosthetic vision in animals with retinal degeneration. *Vision Res*. 2015;111:142–148. <https://doi.org/10.1016/j.visres.2014.09.007>.

9. Stingl K, Bartz-Schmidt KU, Gekeler F, et al. Functional outcome in subretinal electronic implants depends on foveal eccentricity. *Invest Ophthalmol Vis Sci.* 2013;54:7658–7665. <https://doi.org/10.1167/iovs.13-12835>.
10. Ho E, Smith R, Goetz G, et al. Spatiotemporal characteristics of retinal response to network-mediated photovoltaic stimulation. *J Neurophysiol.* 2018;119:389–400. <https://doi.org/10.1152/jn.00872.2016>.
11. Muqit MMK, Hubschman JP, Picaud S, et al. PRIMA subretinal wireless photovoltaic microchip implantation in non-human primate and feline models. *PLoS One.* 2020;15:e0230713. <https://doi.org/10.1371/journal.pone.0230713>.
12. Ho E, Lorach H, Goetz G, et al. Temporal structure in spiking patterns of ganglion cells defines perceptual thresholds in rodents with subretinal prosthesis. *Sci Rep.* 2018;8:3145. <https://doi.org/10.1038/s41598-018-21447-1>.
13. Boinagrov D, Lei X, Goetz G, et al. Photovoltaic pixels for neural stimulation: circuit models and performance. *IEEE Trans Biomed Circuits Syst.* 2016;10:85–97. <https://doi.org/10.1109/TBCAS.2014.2376528>.
14. Ho E, Lei X, Flores T, et al. Characteristics of prosthetic vision in rats with subretinal flat and pillar electrode arrays. *J Neural Eng.* 2019;16:066027. <https://doi.org/10.1088/1741-2552/ab34b3>.
15. Prévot P-H, Geheire K, Arcizet F, et al. Behavioural responses to a photovoltaic subretinal prosthesis implanted in non-human primates. *Nat Biomed Eng.* 2020;4:172–180. <https://doi.org/10.1038/s41551-019-0484-2>.
16. Palanker D, Le Mer Y, Mohand-Said S, et al. Photovoltaic restoration of central vision in atrophic age-related macular degeneration. *Ophthalmology.* 2020;127:1097–1104. <https://doi.org/10.1016/j.ophtha.2020.02.024>.
17. Palanker D, Le Mer Y, Mohand-Said S, Sahel JA. Simultaneous perception of prosthetic and natural vision in AMD patients. *Nat Commun.* 2022;13:513. <https://doi.org/10.1038/s41467-022-28125-x>.
18. Muqit MMK, Mer YL, Holz FG, Sahel JA. Long-term observations of macular thickness after subretinal implantation of a photovoltaic prosthesis in patients with atrophic age-related macular degeneration. *J Neural Eng.* 2022;19:055011. <https://doi.org/10.1088/1741-2552/ac9645>.
19. Lorach H, Wang J, Lee DY, et al. Retinal safety of near infrared radiation in photovoltaic restoration of sight. *Biomed Opt Express.* 2016;7:13–21. <https://doi.org/10.1364/BOE.7.000013>.
20. José PC, Bates DM. *Mixed-Effects Models in S & S-Plus.* New York, NY: Springer Verlag; 2006.
21. R Core Team. R: A Language and Environment for Statistical Computing. Vienna, Austria: R Foundation for Statistical Computing; 2021. <https://www.R-project.org/>.
22. Zrenner E, Bartz-Schmidt KU, Benav H, et al. Subretinal electronic chips allow blind patients to read letters and combine them to words. *Proc Biol Sci.* 2011;278:1489–14897. <https://doi.org/10.1098/rspb.2010.1747>.
23. Luo YH-L, da Cruz L. The Argus® II retinal prosthesis system. *Prog Retin Eye Res.* 2016;50:89–107. <https://doi.org/10.1016/j.preteyeres.2015.09.003>.
24. Humayun MS, Dorn JD, da Cruz L, et al. Interim results from the international trial of Second Sight's visual prosthesis. *Ophthalmology.* 2012;119:779–788. <https://doi.org/10.1016/j.ophtha.2011.09.028>.
25. Stingl K, Bartz-Schmidt KU, Besch D, et al. Subretinal visual implant Alpha IMS – clinical trial interim report. *Vision Res.* 2015;111:149–160. <https://doi.org/10.1016/j.visres.2015.03.001>.
26. Stingl K, Schippert R, Bartz-Schmidt KU, et al. Interim results of a multicenter trial with the new electronic subretinal implant Alpha AMS in 15 patients blind from inherited retinal degenerations. *Front Neurosci.* 2017;11:445. <https://doi.org/10.3389/fnins.2017.00445>.
27. Grzybowski A, Wang J, Mao F, et al. Intraocular vision-improving devices in age-related macular degeneration. *Ann Transl Med.* 2020;8:1549. <https://doi.org/10.21037/atm-20-5851>.
28. Ehrlich JR, Ojeda LV, Wicker D, et al. Head-mounted display technology for low-vision rehabilitation and vision enhancement. *Am J Ophthalmol.* 2017;176:26–32. <https://doi.org/10.1016/j.ajo.2016.12.021>.
29. Sarda SP, Heyes A, Bektas M, et al. Humanistic and economic burden of geographic atrophy: a systematic literature review. *Clin Ophthalmol.* 2021;15:4629–4644. <https://doi.org/10.2147/OPHTH.S338253>.
30. Sivaprasad S, Tschosik EA, Guymer RH, et al. Living with geographic atrophy: an ethnographic study. *Ophthalmol Ther.* 2019;8:115–124. <https://doi.org/10.1007/s40123-019-0160-3>.
31. Künzel SH, Lindner M, Sassen J, et al. Association of reading performance in geographic atrophy secondary to age-related macular degeneration with visual function and structural biomarkers. *JAMA Ophthalmol.* 2021;139:1191–1199. <https://doi.org/10.1001/jamaophthalmol.2021.3826>.
32. Goldberg R, Heier JS, Wykoff CC, et al. Efficacy of intravitreal pegcetacoplan in patients with geographic atrophy: 12-month results from the phase 3 OAKS and DERBY studies. *Invest Ophthalmol Vis Sci.* 2022;63:1500.
33. Holekamp N, Wykoff CC, Schmitz-Valckenberg S, et al. Natural history of geographic atrophy secondary to age-related macular degeneration: results from the prospective proxima A and B clinical trials. *Ophthalmology.* 2020;127:769–783. <https://doi.org/10.1016/j.ophtha.2019.12.009>.
34. Schmitz-Valckenberg S, Nadal J, Fimmers R, et al. Modeling visual acuity in geographic atrophy secondary to age-related macular degeneration. *Ophthalmologica.* 2016;235:215–224. <https://doi.org/10.1159/000445217>.
35. Castaldi E, Cicchini GM, Cinelli L, et al. Visual BOLD response in late blind subjects with Argus II retinal prosthesis. *PLoS Biol.* 2016;14:e1002569. <https://doi.org/10.1371/journal.pbio.1002569>.
36. Wang BY, Chen ZC, Bhuckory M, et al. Electronic photoreceptors enable prosthetic visual acuity matching the natural resolution in rats. *Nat Commun.* 2022;13:6627. <https://doi.org/10.1038/s41467-022-34353-y>.
37. Chen ZC, Wang BY, Kochnev Goldstein A, et al. Photovoltaic implant simulator reveals resolution limits in subretinal prosthesis. *J Neural Eng.* 2022;19:055008. <https://doi.org/10.1088/1741-2552/ac8ed8>.